

# Binary neutron star mergers as the source of the highest energy cosmic rays

Glennys R. Farrar<sup>1, \*</sup>

<sup>1</sup>*Center for Cosmology and Particle Physics, Department of Physics  
New York University, New York, NY 10003, USA*

(Dated: May 21, 2024)

We propose that ultrahigh energy cosmic rays are produced in binary neutron star mergers. Interpreting the highest energy events as r-process nuclei eliminates the need for exotic sources, while the observed near-universal maximum rigidity of ultrahigh energy sources can be understood as due to the uniformity of jets generated by the gravitationally-driven dynamo, given the narrow range of total binary neutron star masses. We discuss evidence for this scenario, and its prediction of coincidences between neutrinos above 10 PeV and gravitational waves.

Keywords:

## Introduction

Major advances in ultrahigh energy cosmic ray (UHECR) observations in the past two decades have led to a much better understanding of their spectrum and composition, but the central question remains: What are the systems responsible for accelerating cosmic rays to the highest observed energies? We argue here that two particularly puzzling features of the observations strongly suggest that extragalactic cosmic rays are produced in binary neutron star (BNS) mergers, with the highest energy events being r-process nuclei such as tellurium. This BNS-merger scenario explains all current observations, within present uncertainties, as we show.

Options for UHECR sources are constrained by the observed rate and energetics, the spectrum and composition, inhomogeneities in arrival directions (dipole and higher multipoles and hotspots), and constraints from extremely high energy events such as the recent Amaterasu particle [1]. Additional crucial facts are that individual accelerators have a nearly universal maximum rigidity, which – under the conventional assumption that the heaviest UHECRs are iron nuclei – requires an entirely different source class to explain the highest energy events [1, 2]. After giving a brief overview, we review the constraints on UHECR sources and note why previously proposed source candidates are problematic in one way or another, motivating the need to seek new possibilities. We show that BNS-mergers can explain all of the observations as of now, and close with a discussion of tests and implications of this scenario.

## Overview

The very large exposures of the Pierre Auger Observatory in Argentina and the Telescope Array in Utah (TA) have resulted in  $\approx 50,000$  events having been recorded above 10 EeV ( $10^{19}$  eV) [3], of which more than 40 are above 100 EeV [4]. At these energies, Galactic cosmic rays (GCRs) make a negligible contribution. The cut-off in the spectrum at the highest energies is due to a combination of limited accelerating-power of the sources

and Greisen-Zatsepin-Kuzmin processing [5–7]. For protons, GZK energy loss is due primarily to inelastic scattering on cosmic microwave background photons. For nuclei, interactions with the CMB and other extragalactic background light cause spallation or breakup; these interactions conserve the energy per nucleon. The rigidity,  $\mathcal{R} \equiv E/Ze$ , where  $E$  is energy and  $Ze$  is charge, is twice the energy per nucleon, for common nuclei except protons, and thus is approximately conserved during propagation.

The observed composition above 10 EeV is consistent with UHECRs being nuclei with a relatively narrow range of rigidities centered on  $\mathcal{R} \approx 4$  EV. (See, e.g., Fig. 4 of [8].) Below 10 EeV lies a transition region where the low end of the extragalactic spectrum overlaps the highest energy Galactic cosmic rays. The light extragalactic component is well-explained as resulting from spallation of primary UHE nuclei as they pass through the environment surrounding the accelerator [9]. The protons' origin as spallation products – revealed by their having a common energy per nucleon rather than rigidity, with respect to other UHECRs – is a key indicator of the validity of this mechanism.

## Constraints on UHECR sources

1. Universal maximum rigidity: Arguably the most puzzling feature of UHECRs is that the spread in nuclear masses appearing at any given energy is so small [10], such that the rigidity spectrum is very narrow – only a factor-few in width. It is to be expected that different nuclei accelerated in an individual source have essentially the same spectrum in rigidity, since known acceleration mechanisms depend only on rigidity and that is preserved during propagation as discussed above. However for source classes proposed up to now, different sources should exhibit different maximum rigidities so that an ensemble of sources would in general have a broad rigidity spectrum, contrary to observations [7]. This problem was systematically investigated in Ref. [11], where it was shown that none of the conventional source can-

didates (blazars, long GRBs, TDEs) have a sufficiently small population variance to yield a distribution of maximum rigidities consistent with the UHECR composition data. (Seyfert galaxies – low luminosity AGN – were found to be marginally compatible within the scope of the analysis but vulnerable to exclusion when all sources of variance are taken into account [11].)

**2. The Hillas criterion:** A candidate UHECR source must be capable of accelerating UHECRs to the observed rigidity. The characteristic size of the accelerating region,  $R$ , must be large enough to confine the UHECR – i.e.,  $R$  cannot be significantly smaller than the Larmor radius of the cosmic ray. This leads to the *Hillas criterion* relating the maximum rigidity to which UHECRs are accelerated to the size and field strength in the source:

$$\mathcal{R}_{\max, \text{EV}} \lesssim 3 \times 10^{-11} \Gamma_{\text{jet}} R_{\text{km}} B_{\text{G}} , \quad (1)$$

where  $B_{\text{G}}$  is the magnetic field strength of the jet in Gauss,  $\Gamma_{\text{jet}}$  is its relativistic boost factor and  $R_{\text{km}}$  is the characteristic size of the confinement region in km; see, e.g., [12]. Since the Poynting luminosity is proportional to the cross-sectional area times  $\vec{E} \times \vec{B}$ , the Hillas condition (1) on  $RB$  means that the minimum Poynting luminosity of the jet is determined, independently of  $R$  and  $B$  separately. This implies a condition on the (isotropic equivalent) total power of a jet capable of accelerating CRs to a rigidity  $\mathcal{R}_{\max, \text{EV}}$ ; e.g.. from [12]:

$$\mathcal{L}_{\text{bol}} > \frac{c}{6} \Gamma_{\text{jet}}^4 B^2 R^2 \approx 10^{41} \Gamma_{\text{jet}}^2 \mathcal{R}_{\max, \text{EV}}^2 \text{ erg/s} . \quad (2)$$

If UHECRs were protons so  $\mathcal{R} = E$ , this would be a very stringent requirement and rule out all but extremely luminous sources.

**3. Total UHECR energy injection:** In addition to the conditions (1) and (2), a source class capable of explaining all UHECRs must account for the observed total flux of UHECRs. Since UHECRs lose energy during propagation due to GZK processes, a steady replenishment is required. The volumetric energy-injection rate for UHECRs above 10 EeV is [13]

$$\dot{\mathcal{Q}} = 6 \times 10^{44} \text{ erg Mpc}^{-3} \text{ yr}^{-1} . \quad (3)$$

(The low energy limit chosen to define  $\dot{\mathcal{Q}}$  only matters at the  $\mathcal{O}(1)$  level since the spectrum emerging from the source is hard,  $dN/dE \sim E^{-p}$  with  $p \lesssim 1$  [7]; the 10 EeV threshold adopted here avoids contamination by Galactic cosmic rays.) For continuous sources, Eq. (3) constrains the product of the number density of sources times their mean luminosity in UHECRs:  $n_S \mathcal{L}_{\text{UCR}} = \dot{\mathcal{Q}}$ . For transient sources, the constraint is  $\Gamma_S \mathcal{E}_{\text{UCR}} = \dot{\mathcal{Q}}$ , where  $\Gamma_S$  is the volumetric rate of the transient sources and  $\mathcal{E}_{\text{UCR}}$  is the total energy in UHECRs above the specified threshold, produced in an average transient event.

**4. Number density of contributing sources:** The observations of UHECR arrival directions are very constraining on candidate source classes, even without individual sources having been identified. Auger finds that the higher multipoles beyond dipole are consistent with those of an isotropic distribution; this upper limit on small and intermediate scale inhomogeneities was used in Ref. [8] to constrain the density of UHECR sources to

$$n_S \gtrsim 10^{-3.5} \text{ Mpc}^{-3} . \quad (4)$$

This number density constraint disfavors rare continuous sources such as blazars, powerful AGN and starburst galaxies, apart from a marginally viable narrow window for sufficiently high extragalactic magnetic smearing. Figure 1 in the Appendix reproduced from [8] displays the constraint.

For transients, the constraint (4) is on the effective source density  $n_S^{\text{eff}} \equiv \Gamma_S \tau$ , where  $\Gamma_S$  is the volumetric rate of transients producing UHECRs above the energy threshold and  $\tau$  is the mean arrival time spread of the UHECRs from a transient event within the GZK horizon. Due to UHECR deflections in the magnetic fields between source and detector, the UHECRs arriving at the Milky Way are spread over an angle  $\psi$  and arrive with time delay up to  $\tau$  [14]:

$$\psi \approx 30^\circ \beta_{\text{EGMF}} \sqrt{D_{\text{Mpc}} / \mathcal{R}_{\text{EV}}} \quad (5)$$

$$\tau \approx 0.14 (D_{\text{Mpc}} \beta_{\text{EGMF}} / \mathcal{R}_{\text{EV}})^2 \text{ Myr} , \quad (6)$$

where the extragalactic magnetic smearing parameter is

$$\beta_{\text{EGMF}} \equiv B_{\text{EGMF}} / \text{nG} \sqrt{L_c / \text{Mpc}} . \quad (7)$$

Commonly adopted estimates are  $B_{\text{EGMF}} \approx 1$  nG, and  $L_c$  in the range of 10 kpc to 1 Mpc, giving  $\beta_{\text{EGMF}}$  from 0.1 to 1. For jetted sources, continuous or transient, the contributing source density is reduced relative to the actual density by the fraction  $f_{\text{contrib}}$ , which may be crudely estimated as  $f_{\text{contrib}} \approx \sin(\sqrt{\delta_j^2 + \psi^2})$  with  $\delta_j$  being the jet opening angle. The mean source distance of UHECRs above 32 EeV is 70 Mpc [8], so for a 2-sided jet whose opening angle is  $10^\circ$  the sky-averaged value of  $f_{\text{contrib}}$  ranges from 0.2 for small  $\beta_{\text{EGMF}}$  to 1 for  $\beta_{\text{EGMF}} \gtrsim 0.6$ . Long GRBs and visibly jetted TDEs – those TDEs whose jets are visible almost immediately – are disfavored as the exclusive source of UHECRs by this criterion, being marginally possible only if the mean  $\beta_{\text{EGMF}}$  is near its maximum allowed value [8]; see Fig. 1 in the Appendix.

**5. Amaterasu Event:** The very energetic cosmic ray Amaterasu detected by TA [15] provides direct evidence that at least some UHECRs are produced by transient events, as demonstrated in [2]. In brief, because of its high energy, GZK energy losses during propagation severely restrict the distance of Amaterasu’s source. Its nominal energy, in view of its likely composition, is

$E_{\text{nom}} = (212 \pm 25)$  EeV for which the source must be within  $\approx 13$  Mpc [2]. Taking into account the uncertainties in energy and composition, Ref. [2] backtracked Amaterasu through the Galactic magnetic field using the recent UF23 suite of GMF models [16], which capture the uncertainty in GMF deflections. The maximum source volume contains only ordinary galaxies and a few low-luminosity AGNs, suggesting that Amaterasu was created by a transient event in an otherwise ordinary galaxy.

### Source candidates

Early favorite candidate UHECR sources were the jets found in powerful AGN or long GRBs [17, 18]. However both are now essentially excluded, except as the source of a small fraction of events, by (i) the source density requirement,  $n_S \gtrsim 10^{-3.5} \text{ Mpc}^{-3}$ , (ii) the standard source requirement, and (iii) the absence of those sources in the Amaterasu source volume. An additional problem for long GRBs is that they cannot account for the volumetric energy injection rate,  $\dot{Q}$ , unless the UHECR energy in GRBs exceeds the energy in gamma rays by two orders of magnitude [12].

AGN minimally satisfying the bolometric luminosity condition to accelerate to 5 EV,  $\mathcal{L}_{\text{bol}} \gtrsim 10^{42.5} \text{ erg/s}$ , may be marginally consistent with the number density requirement – c.f., the AGN luminosity function in [19]. However still lower luminosity AGN are much more abundant – Zaw et al. [20], finds that 40% of the SDSS galaxies out to  $z = 0.07$  are either broad-line AGN or satisfy the Kewley narrow-line AGN criterion – so the narrow rigidity distribution of UHECRs (the standard reach condition) is implausible for continuous AGN; see also [11].

Another possibility for UHECR acceleration was suggested in [12]: short-lived but powerful jets in giant flares of otherwise low-luminosity AGNs, produced by a disk instability or accretion event, or the jets of tidal disruption events (TDEs) when a star passes close enough to a supermassive black hole to be shredded, forming an accretion disk and sometimes a jet. TDEs were subsequently discovered [21] and the rate found to be potentially sufficient [22]. Many TDEs have now been detected, and several spatio-temporal correlations between TDEs and high energy astrophysical neutrinos have been reported [23–25]; see [26] for a recent discussion. However it remains to be seen whether jetted TDEs are sufficiently abundant to explain the smoothness of the UHECR arrival direction distribution (4) and the energy injection requirement (3). Extreme-jetted TDEs – the rare cases when a powerful jet is almost immediately apparent – are too rare [8] – but recent observations and theory suggest that jets may only become visible through radio emission a year or more after the merger event, so the jury is out on whether jetted TDEs could by themselves produce all the UHECRs. However even if capable TDEs are sufficiently abundant, the near-universal maximum rigidity of UHECR sources is a serious challenge to the

TDE scenario because TDEs are a very diverse population unlikely to have a narrow distribution of acceleration capability.

A distinctly different but appealing proposal is that UHECRs are accelerated in accretion shocks of galaxy clusters and filaments [27]. However the Amaterasu event’s origination in a region not containing a galaxy cluster, requires that mild as well as massive shocks accelerate to the highest energies, which seemingly would imply a very broad distribution of source maximum rigidities, contrary to the data.

### Binary Neutron Star mergers & UHECRs

Binary neutron star mergers provide a natural rationale for the near-universal maximum rigidity: Gravity and angular momentum govern the dynamo process which generates the jets, and the range of total binary mass is very narrow with just a 5% spread around the mean [53]. Thus the jets produced in BNS mergers can be expected to be nearly the same from one merger to another [54]. The very high-resolution GR-MHD simulation of the merger of two  $1.35 M_{\odot}$  neutron stars in Ref. [28] demonstrates that dynamo action produces a pair of jets with fields in excess of  $10^{15}$  G on multi-km length scales, easily satisfying the Hillas criterion.

Having motivated that BNS mergers can have a common maximum rigidity at the required factor-few level, we turn to the effective source density and global UHECR energy injection requirements. Both of these depend on the BNS merger rate. Estimating the rate depends on assumptions, so it is reassuring that two different methods give similar results, albeit presently with large uncertainties. The LIGO-Virgo-Kagra collaboration’s conservative range on the BNS merger rate is  $10\text{--}1700 \text{ Gpc}^{-3} \text{ yr}^{-1}$  [29]. This is compatible with the recent detailed study of the afterglows of 29 short GRBs [30] which finds, using events with well-measured opening angles, a beaming-corrected short GRB rate of  $1786_{-1507}^{+6346} \text{ Gpc}^{-3} \text{ yr}^{-1}$ . Below, we take the BNS merger rate to be  $\Gamma_3 \times 10^3 \text{ Gpc}^{-3} \text{ yr}^{-1}$ .

The contributing source density constraint is readily satisfied by BNS mergers, as follows. Using Eq. (6), with mean source distance of 70 Mpc and mean rigidity 4.5 EV for the more demanding 32 EeV threshold [8] requires  $n_{\text{eff}} \gtrsim 34 \Gamma_3 \beta_{\text{EGMF}}^2 \text{ Mpc}^{-3}$ . The opening angle of the jet is  $12^\circ$  [28] so  $f_{\text{contrib}} \approx 0.2 - 1$  and the effective source density requirement derived in [8],  $n_{\text{eff}} \gtrsim 10^{-3.5} \text{ Mpc}^{-3}$ , is satisfied as long  $\beta_{\text{EGMF}}^2 \Gamma_3 f_{\text{contrib}} \gtrsim 10^{-5}$ . The conservative lower bound on the BNS merger rate from gravitational waves gives  $\Gamma_3 > 10^{-2}$  [29] so with  $f_{\text{contrib}} \approx 0.6$ , the observed source density requirement is satisfied as long as  $\beta_{\text{EGMF}} \gtrsim 0.04$ , as is expected.

Accounting for the entire observed UHECR energy injection rate is also possible within present uncertainties. The simulation of Ref. [28] finds a Poynting luminosity in excess of  $10^{51} \text{ erg/s}$  and a magnetically-driven wind

with kinetic energy  $5 \times 10^{50}$  erg, when the simulation ends about 150 ms post-merger. For a typical 1s duration, this suggests an energy budget for UHECRs of  $1.5 \epsilon_{1.5} \times 10^{51}$  erg, giving the observed  $\dot{Q}$  if  $\epsilon_{1.5} \Gamma_3 = 0.4$ , comfortably in the constrained range. Simulations of particle acceleration in BNS merger jets are needed, especially through the recently-appreciated mechanism of plasmoid-mediated magnetic reconnection [31–33] which is expected to be dominant in Poynting-flux dominated outflows, because [28] does not take into account particle acceleration and feedback. Simulations are also needed to check that photons do not overly dissociate nuclei; [34] showed this is not a problem for long GRBs and it is likely also the case for BNS merger jets.

### Tests and implications

R-process UHECRs and the highest energy CRs: In the BNS-merger scenario, most UHECRs are typical nuclei of the ambient medium around the binary, which get swept up in the jets and accelerated. They may be spallated to some extent while escaping through the medium surrounding the accelerator and during extragalactic propagation [9]. In addition, a contribution of r-process elements can be expected. Half of all r-process nuclei are produced by nucleosynthesis in binary neutron star mergers which is generally thought to take place in ejecta in the equatorial plane of the merger [35]. Occasionally, a heavy nucleus can migrate into a jet and be accelerated, enhancing the fraction of r-process elements in UHECRs relative to the Galactic average. The masses of r-process nuclei peak around  $A = 130$  (Te-Xe;  $Z = 52-54$ ) and  $A = 195$  (Pt;  $Z = 78$ ); see [36] for a recent review. Taking  $\mathcal{R} \approx 4.5 \pm 0.5$  EV to approximate the mean universal rigidity [8], the energies of these peak r-process nuclei after acceleration in the source are  $E \approx 240 \pm 25$  EeV and  $350 \pm 40$  EeV.

The proposal here that UHECRs originate in BNS mergers, and hence naturally contain some component of r-process elements, provides the first compelling, non-exotic explanation for the highest energy UHECR ever recorded: the Fly’s Eye “OMG” event [37]. Its energy was originally estimated to be  $320 \pm 90$  EeV. Simply rescaling that value using the modern air fluorescence yield [38] implies a more accurate estimated energy assignment is  $250 \pm 70$  EeV; a more detailed re-analysis updating the pressure dependence is warranted. As we now show, the Fly’s Eye data is comfortably explained as an r-process nucleus for energy assignments in this range. A similar analysis applies to the Amaterasu particle.

Since the rigidity range is very narrow, we can estimate the charge of the OMG event for any given energy using the mean rigidity of 4.5 EV [8]. This results in an estimated charge of  $(56 \pm 15)$  ( $\frac{4.5}{\mathcal{R}}$ ) for  $E = 250 \pm 70$  EeV, suggesting this event originated near the Te-Xe r-process peak, since the charge loss of heavy nuclei in propagation is small [55].

The depth-of-shower-maximum of the OMG event was measured to be  $X_{\max} = 815_{-53}^{+60} \text{ g cm}^{-2}$  including both systematic and statistical uncertainties [37]. We compare this to the expectations under the illustrative interpretation of  $(A, E) = (130, 250 \text{ EeV})$ . The predicted  $X_{\max}$  for Fe at the nominal energy is  $800 \text{ g cm}^{-2}$ , using Sybill23d to simulate the shower development. The depth-of-shower-maximum shifts with nuclear mass and incident cosmic ray energy as  $d\langle X_{\max} \rangle / d\log_{10} A \approx -d\langle X_{\max} \rangle / d\log_{10} E \approx -60 \text{ g cm}^{-2}$  [39]. For  $E = 250$  EeV the tellurium identification predicts  $X_{\max} = 773 \text{ g cm}^{-2}$ , consistent with observation within  $1\sigma$ .

In sum, the Fly’s Eye data on both the energy deposit and the depth of shower maximum of the OMG event fit well with its being an ultrahigh energy cosmic ray nucleus in the tellurium peak of r-process nucleosynthesis. Thus the very existence of this event can be considered tentative evidence of the binary neutron star merger origin of UHECRs. (If the maximum UHECR charge is 26, which appears to have been universally assumed up to now, the Fly’s Eye event must either have an unknown exotic origin or have a rigidity  $\mathcal{R} \gtrsim 10$  EV: more than twice that of other UHECRs. With such a high rigidity, by Eq. (3) its source should have at least an order of magnitude higher luminosity than the average source. For additional perspectives on this event see [40–43].) With a large enough sample of well-measured events above 150 EeV, as may be possible with proposed future detectors such as GCOS [44], the contributions of different r-process nuclei to extreme energy CRs could be mapped out.

EHE neutrinos associated with BNS mergers: As noted in the Introduction, the light composition of UHECRs below the ankle is nicely explained as due to interactions of higher-mass UHECRs with photons or gas in the environment of the accelerator [9]. These interactions produce a population of neutrinos with peak energy of about 20 PeV [45]; see Fig. 3 in the Appendix reproduced from [45]. In the BNS merger scenario for UHECR production, neutrinos in the 20 PeV peak energy range are produced by UHECRs interacting on their way out of the source environment. Thus every neutrino detected in this energy range should be accompanied by the gravitational wave (GW) produced by the neutron star merger. Since the cosmic ray, GW and neutrino travel at essentially the speed of light, the arrival time delay at observation between the GW and neutrino is mainly due to the extra path length of the UHECR relative to the GW on account of its magnetic deflections prior to the interaction in the source environment which produces the neutrino. This needs to be estimated in order to determine the relevant window for spatial-temporal coincidences between gravitational waves and neutrinos in the 20 PeV peak. From Fig. 24 of [46], the sensitivity of IceCube-Gen2 to diffuse astrophysical neutrinos after 10 years of opera-

tion should be an order of magnitude below the predicted peak flux [45]. Moreover according to Ref. [47], the efficiency for detection of a BNS merger within  $z = 2$  at  $\text{SNR} \geq 10$  should be 40% with the “4020ET” GW detection network. So, coincident observations of a BNS merger and a neutrino in this very high energy population, which would confirm the BNS origin of UHECRs, looks promising with next-generation detectors.

### Summary

We have proposed that binary neutron star mergers are the source of ultrahigh energy cosmic rays. Due to the very narrow range of total mass of binary neutron stars and the fact that the magnetic field in the jet is produced by a dynamo whose energy source is gravitational, it is plausible that UHECR production is almost universal from one merger event to another. This can explain the small source-to-source variation in UHECR maximum rigidity, which is a severe challenge to conventional source types as demonstrated in [11]. The observed narrow range of maximum source rigidities indicates that previously considered source types, which have a wide range of maximum rigidities, can make at most a subdominant contribution to UHECR production. The rate of binary neutron star mergers and power of their jets are compatible with BNS mergers accounting for all UHECRs within present constraints, but more precise determinations could challenge this scenario as well.

Since neutron star mergers are the site of r-process nucleosynthesis, our proposal suggests the existence of UHECRs with a composition significantly heavier than Fe. An immediate success of this scenario is that the Fly’s Eye “OMG” event is naturally explained as an r-process nucleus in the tellurium peak, rather than being an extreme outlier requiring a uniquely powerful accelerator or exotic origin. The same applies to the Amaterasu particle if its true energy is close to its nominal value. In the future, UHECR data should be interpreted allowing for the possibility of a component of r-process nuclei, and codes to model UHECR energy losses during extragalactic propagation should be extended to include r-process nuclei.

### Acknowledgments

I am grateful to T. Bister, M. Muzio and M. Unger for fruitful collaborations and for valuable input which has stimulated and enriched the work presented here. I also thank B. Dawson, M. Unger and A. A. Watson for discussions of an updated interpretation of the Fly’s Eye event, and I much appreciate helpful information from L. Comisso, M. Mapelli, A. MacFadyen and B. Metzger. This research has been supported by the National Science Foundation PHY-2013199.

## APPENDIX A: AMATERASU AND ANDROMEDA

The source locus of TA’s Amaterasu event is devoid of distinctive source candidates [2], but does contain our neighbor Andromeda (M31), a galaxy of comparable mass to the Milky Way at a distance of 765 kpc. In a scenario such as ours where every galaxy hosts UHECR production in proportion to its BNS merger rate, M31 should be an *a priori* relatively powerful source. This raises the question of whether – were M31 the source of Amaterasu – could that somehow be discovered and relic evidence of the event investigated.

To gauge the likelihood that a BNS merger in M31 could have produced Amaterasu, we calculate the expected number of BNS mergers in M31 contributing to UHECRs detected today. Analysis of Milky Way double-NS systems leads to an estimated BNS merger rate in the Milky Way of  $32_{-9}^{+19} \text{ Myr}^{-1}$  [48], which should be applicable to M31 given its similarities to our Galaxy. Two additional factors enter the probability of observing a UHECR today from a BNS merger in M31 some time in the past: the arrival-time spread,  $\tau$ , and the fraction of UHECRs reaching the Milky Way,  $f_{\text{contrib}}$ , discussed below Eq. (6); both depend on the intervening magnetic fields through the smearing factor  $\beta$ .

The strength and coherence length of the random magnetic field within the Local Group has not been directly constrained. Using stacked observations of filaments Ref. [49] estimates the average random field strength at  $z = 0$  to be  $B_{\text{rand}} \approx (8 - 26) \text{ nG} (\delta_g/10)^{2/3}$ , where  $\delta_g$  is the gas density relative to the cosmic mean gas density. But it is not clear what to take for the path-averaged value of  $\delta_g$ . Amaterasu’s trajectory would likely have passed through the stellar disks of both M31 and the Milky Way, where the random field strength reaches  $\mu\text{G}$  levels, but only over a length scale of 10’s kpc. Writing  $\beta_{\text{M31}} = 6 (B_{\text{LG}}/30 \text{ nG}) \sqrt{L_{\text{c,LG}}/40 \text{ kpc}}$ , gives an estimated arrival time spread  $\tau_{\text{M31}} = 184 \text{ kyr} (\beta_{\text{M31}}/6)^2$  and  $f_{\text{contrib}} \approx 1$ , implying there is a reasonable chance that a BNS merger in M31 occurred recently enough to have produced Amaterasu.

Someday it might become possible to identify sites of BNS mergers through localized over-densities of r-process elements and – very futuristically – conceivably determine the orientation of the jet from the plane of r-process enhancement. In a most optimistic world in which magnetic deflections en route from M31 are small enough for the event to have reached Earth with little angular dispersion, the UHECR arrival direction to the Galaxy would constrain the direction of the jet, whose opening angle is  $\approx 10^\circ$  [28], thereby potentially implying the geometry of r-process enhancement. Otherwise, there would be nothing distinctive to argue that a BNS

merger relic was associated with production of Amaterasu. (Note that deflection in the Milky Way has been accounted for in the discussion of [2].)

## APPENDIX B: SOME FIGURES FROM CITED PAPERS

For the convenience of the reader, we reproduce here a few relevant figures from the literature.

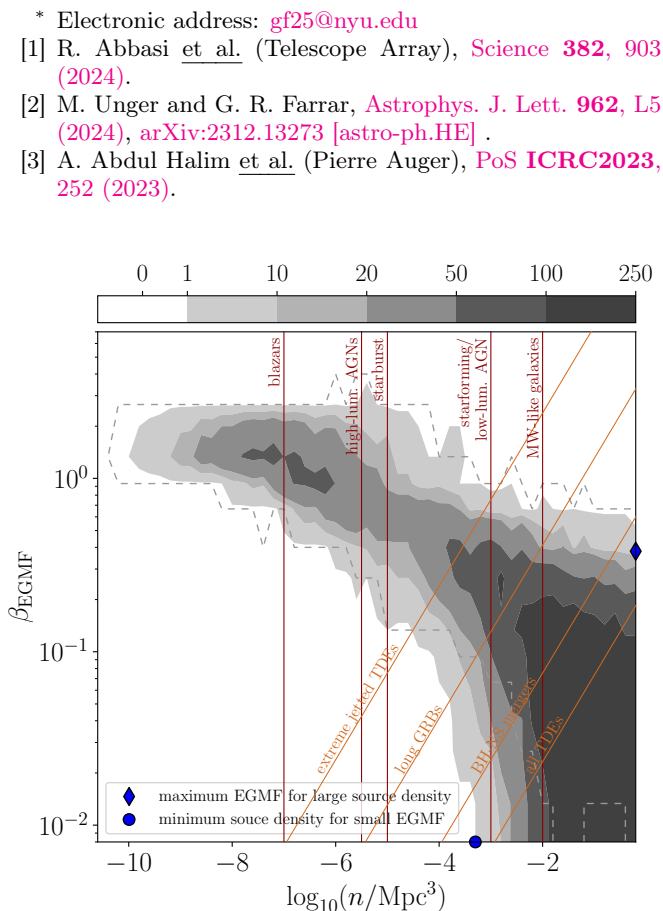


FIG. 1: Figure 11 from [8] showing combined constraints on the the source number density  $n$  and EGMF smearing parameter  $\beta_{\text{EGMF}} \equiv B/nG \sqrt{L_c}/\text{Mpc}$ ; dark grey regions are favored. The intensity bar shows the number of simulations out of 1000 total that have both a sufficiently large dipole and sufficiently small higher moments. The white region is excluded at more than 99% CL. Characteristic estimates of the number densities of some steady source candidates are shown with red lines, and indicative locii of transient source candidates and references. The line labeled NS-BH mergers corresponds to  $\Gamma_3 = 0.03$ . The effect of beaming due to a limited jet opening angle is not included.

- [4] A. Abdul Halim *et al.* (Pierre Auger), *Astrophys. J. Suppl.* **264**, 50 (2023), [arXiv:2211.16020 \[astro-ph.HE\]](https://arxiv.org/abs/2211.16020).
- [5] K. Greisen, *Phys. Rev. Lett.* **16**, 748 (1966).
- [6] G. T. Zatsepin and V. A. Kuzmin, *JETP Lett.* **4**, 78 (1966).
- [7] A. A. Halim *et al.* (Pierre Auger), *JCAP* **05**, 024, [arXiv:2211.02857 \[astro-ph.HE\]](https://arxiv.org/abs/2211.02857).
- [8] T. Bister and G. R. Farrar, (2023), [arXiv:2312.02645 \[astro-ph.HE\]](https://arxiv.org/abs/2312.02645).
- [9] M. Unger, G. R. Farrar, and L. A. Anchordoqui, *Phys.Rev.* **D92**, 123001 (2015), [arXiv:1505.02153 \[astro-ph.HE\]](https://arxiv.org/abs/1505.02153).
- [10] A. Aab *et al.* (Pierre Auger), *Phys. Rev. D* **90**, 122006 (2014), [arXiv:1409.5083 \[astro-ph.HE\]](https://arxiv.org/abs/1409.5083).
- [11] D. Ehlert, F. Oikonomou, and M. Unger, *Phys. Rev. D* **107**, 103045 (2023), [arXiv:2207.10691 \[astro-ph.HE\]](https://arxiv.org/abs/2207.10691).
- [12] G. R. Farrar and A. Gruzinov, *Astrophys. J.* **693**, 329 (2009), [arXiv:0802.1074](https://arxiv.org/abs/0802.1074).
- [13] M. S. Muzio, G. R. Farrar, and M. Unger, *Phys. Rev. D* **105**, 023022 (2022), [arXiv:2108.05512 \[astro-ph.HE\]](https://arxiv.org/abs/2108.05512).
- [14] A. Achterberg, Y. A. Gallant, C. A. Norman, and D. B. Melrose, (1999), [arXiv:astro-ph/9907060](https://arxiv.org/abs/astro-ph/9907060).
- [15] R. Abbasi *et al.* (Telescope Array), *Science* **382**, 903 (2024).
- [16] M. Unger and G. R. Farrar, (2023), [arXiv:2311.12120](https://arxiv.org/abs/2311.12120).
- [17] M. Vietri, *Astrophys. J.* **453**, 883 (1995), [arXiv:astro-ph/9506081 \[astro-ph\]](https://arxiv.org/abs/astro-ph/9506081).
- [18] E. Waxman, *Phys. Rev. Lett.* **75**, 386 (1995), [astro-ph/9505082](https://arxiv.org/abs/astro-ph/9505082).
- [19] Duras, F., Bongiorno, A., Ricci, F., Piconcelli, E., Shankar, F., Lusso, E., Bianchi, S., Fiore, F., Maiolino, R., Marconi, A., Onori, F., Sani, E., Schneider, R., Vignali, C., and La Franca, F., *A&A* **636**, A73 (2020).
- [20] I. Zaw, Y.-P. Chen, and G. R. Farrar, *Astrophys. J.* **872**, 134 (2019), [arXiv:1902.03799 \[astro-ph.GA\]](https://arxiv.org/abs/1902.03799).
- [21] S. van Velzen, G. R. Farrar, S. Gezari, N. Morrell, D. Zaritsky, L. Ostman, M. Smith, J. Gelfand, and A. J. Drake, *Astrophys. J.* **741**, 73 (2011), [arXiv:1009.1627 \[astro-ph.CO\]](https://arxiv.org/abs/1009.1627).
- [22] S. van Velzen and G. R. Farrar, *Astrophys. J.* **792**, 53 (2014), [arXiv:1407.6425 \[astro-ph.GA\]](https://arxiv.org/abs/1407.6425).
- [23] R. Stein *et al.*, *Nature Astron.* **5**, 510 (2021), [arXiv:2005.05340 \[astro-ph.HE\]](https://arxiv.org/abs/2005.05340).
- [24] S. Reusch, R. Stein, M. Kowalski, S. van Velzen, A. Franckowiak, C. Lunardini, K. Murase, W. Winter, J. C. A. Miller-Jones, M. M. Kasliwal, M. Gilfanov, S. Garrappa, V. S. Paliya, T. Ahumada, S. Anand, C. Barbarino, E. C. Bellm, V. Brinnel, S. Buson, S. B. Cenko, M. W. Coughlin, K. De, R. Dekany, S. Frederick, A. Gal-Yam, S. Gezari, M. Giroletti, M. J. Graham, V. Karambelkar, S. S. Kimura, A. K. H. Kong, E. C. Kool, R. R. Laher, P. Medvedev, J. Necker, J. Nordin, D. A. Perley, M. Rigault, B. Rusholme, S. Schulze, T. Schweyer, L. P. Singer, J. Sollerman, N. L. Strotjohann, R. Sunyaev, J. van Santen, R. Walters, B. T. Zhang, and E. Zimmerman, *Phys. Rev. Lett.* **128**, 221101 (2022), [arXiv:2111.09390 \[astro-ph.HE\]](https://arxiv.org/abs/2111.09390).
- [25] N. Jiang, Z. Zhou, J. Zhu, Y. Wang, and T. Wang, *Astrophys. J. Lett.* **953**, L12 (2023), [arXiv:2307.16667 \[astro-ph.HE\]](https://arxiv.org/abs/2307.16667).
- [26] T. Piran and P. Beniamini, *JCAP* **11**, 049, [arXiv:2309.15644 \[astro-ph.HE\]](https://arxiv.org/abs/2309.15644).
- [27] P. Simeon, N. Globus, K. S. S. Barrow, and R. Blandford,

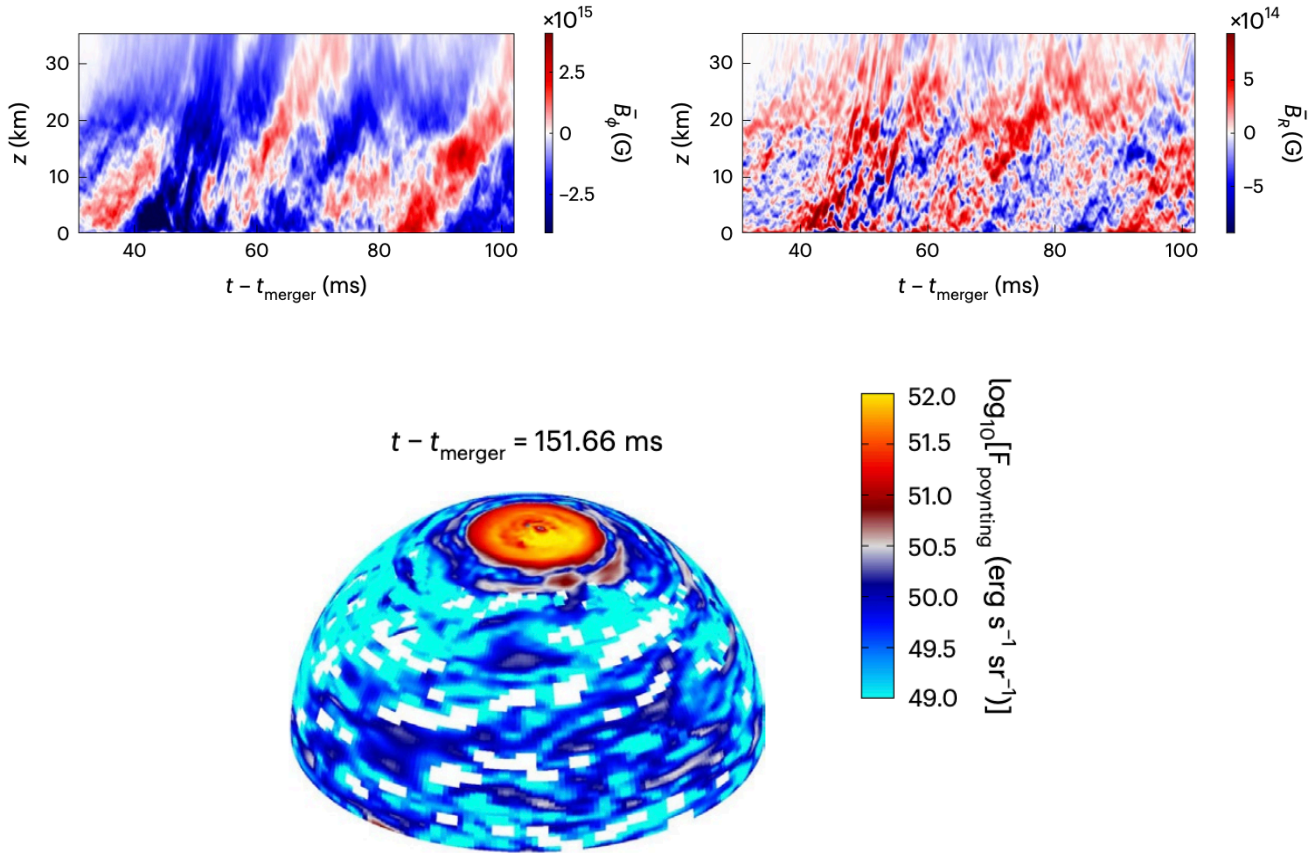


FIG. 2: (top row) The azimuthal and radial fields as a function of distance, from Fig. 3 of [28]; (bottom) the Poynting flux on a sphere at 500 km, 150 ms after the merger, from Fig. 4 of [28].

- Pos **ICRC2023**, 369 (2023).
- [28] K. Kiuchi, A. Reboul-Salze, M. Shibata, and Y. Sekiguchi, (2023), [arXiv:2306.15721 \[astro-ph.HE\]](#).
- [29] R. Abbott et al. (KAGRA, VIRGO, LIGO Scientific), *Phys. Rev. X* **13**, 041039 (2023), [arXiv:2111.03606 \[gr-qc\]](#).
- [30] A. Rouco Escorial, W. Fong, E. Berger, T. Laskar, R. Margutti, G. Schroeder, J. C. Rastinejad, D. Cornish, S. Popp, M. Lally, A. E. Nugent, K. Paterson, B. D. Metzger, R. Chornock, K. Alexander, Y. Cendes, and T. Eftekhari, *Astrophys. J.* **959**, 13 (2023), [arXiv:2210.05695 \[astro-ph.HE\]](#).
- [31] L. Comisso and L. Sironi, *Astrophys. J.* **886**, 122 (2019), [arXiv:1909.01420 \[astro-ph.HE\]](#).
- [32] H. Zhang, L. Sironi, and D. Giannios, *Astrophys. J.* **922**, 261 (2021), [arXiv:2105.00009 \[astro-ph.HE\]](#).
- [33] X. Li, F. Guo, Y.-H. Liu, and H. Li, *The Astrophysical Journal Letters* **954**, L37 (2023).
- [34] B. D. Metzger, D. Giannios, and S. Horiuchi, *MNRAS* **415**, 2495 (2011), [arXiv:1101.4019 \[astro-ph.HE\]](#).
- [35] D. Kasen, B. Metzger, J. Barnes, E. Quataert, and E. Ramirez-Ruiz, *Nature* **551**, 80 (2017), [arXiv:1710.05463 \[astro-ph.HE\]](#).
- [36] J. J. Cowan, C. Sneden, J. E. Lawler, A. Aprahamian, M. Wiescher, K. Langanke, G. Martínez-Pinedo, and F.-K. Thielemann, *Rev. Mod. Phys.* **93**, 015002 (2021).
- [37] D. J. Bird et al., *Astrophys. J.* **441**, 144 (1995), [arXiv:astro-ph/9410067 \[astro-ph\]](#).
- [38] M. Ave et al. (AIRFLY), *Astropart. Phys.* **42**, 90 (2013), [arXiv:1210.6734 \[astro-ph.IM\]](#).
- [39] K.-H. Kampert and M. Unger, *Astropart. Phys.* **35**, 660 (2012), [arXiv:1201.0018 \[astro-ph.HE\]](#).
- [40] J. W. Elbert and P. Sommers, *Astrophys. J.* **441**, 151 (1995).
- [41] M. Risse, P. Homola, D. Gora, J. Pekala, B. Wilczynska, and H. Wilczynski, *Astropart. Phys.* **21**, 479 (2004), [arXiv:astro-ph/0401629](#).
- [42] R. B. Gnatyk, Y. N. Kudrya, and V. I. Zhdanov, *Advances in Astronomy and Space Physics* **6**, 41 (2016).
- [43] T. Fitoussi, G. Medina-Tanco, and J.-C. D’Olivo, *JCAP*

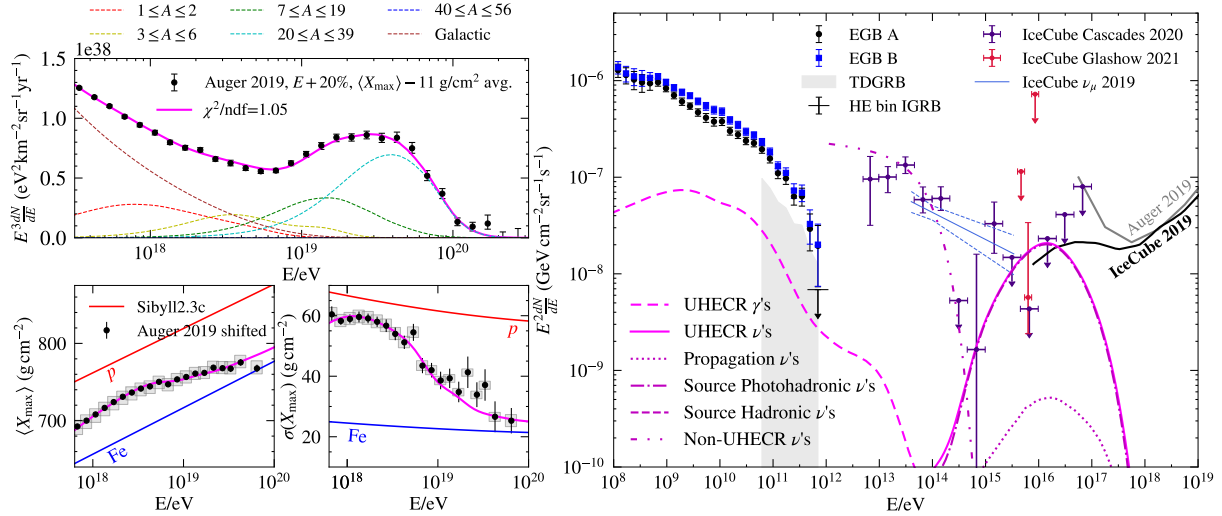


FIG. 3: Figure 1 from [13], extending the analysis of [9]. **Left:** The CR predictions for spectrum (top) and composition (bottom) compared to shifted Auger observations. **Right:** The neutrino and gamma-ray predictions for this model (solid and dashed lines, respectively). The total neutrino flux due to UHECRs (“UHECR  $\nu$ ’s”, solid magenta) is broken down by origin: UHECR interactions during extragalactic propagation (“Propagation  $\nu$ ’s”, dotted dark magenta), UHECR photohadronic and hadronic interactions in the source (“Source  $\nu$ ’s”, dot-dashed and dashed dark magenta, respectively). Neutrinos originating from a source other than UHECRs (“Non-UHECR  $\nu$ ’s”, dot-dot-dashed dark magenta) are also shown. The observed and inferred values of the extragalactic gamma-ray flux, astrophysical neutrino fluxes, flux measurements from the Glashow event, and upper-bounds on the EHE cosmic neutrino flux from IceCube (black) and Auger (grey) are shown. See [13] for details.

01, 042, arXiv:1906.11170 [astro-ph.HE] .

- [44] J. R. Hörandel (GCOS), PoS **ICRC2021**, 027 (2021), arXiv:2203.01127 [astro-ph.HE] .
- [45] M. S. Muzio, G. Farrar, and M. R. Unger, Phys. Rev. D to be submitted (2021).
- [46] [https://urldefense.com/v3/\\_\\_https://icecube-gen2.wisc.edu/science/publications/tdr/\\_\\_;!!DZ3fjg!6NZ5v26I9gwhIP05-14KWTTb-JIildymaQRXBFOooXDZ16djGbkMzNb4W60kqzabA0ZZKCXme8pL-VA\\$](https://urldefense.com/v3/__https://icecube-gen2.wisc.edu/science/publications/tdr/__;!!DZ3fjg!6NZ5v26I9gwhIP05-14KWTTb-JIildymaQRXBFOooXDZ16djGbkMzNb4W60kqzabA0ZZKCXme8pL-VA$), IceCube-Gen2 Technical Design Report, Tech. Rep. (Ice Cube Collaboration).
- [47] I. Gupta et al., (2023), arXiv:2307.10421 [gr-qc] .
- [48] K. Grunthal, M. Kramer, and G. Desvignes, Monthly Notices of the Royal Astronomical Society **507**, 5658 (2021).
- [49] E. Carretti, S. P. O’Sullivan, V. Vacca, F. Vazza, C. Gheller, T. Vernstrom, and A. Bonafede, MNRAS **518**, 2273 (2023), arXiv:2210.06220 [astro-ph.CO] .
- [50] F. Özel and P. Freire, ARAA **54**, 401 (2016), arXiv:1603.02698 [astro-ph.HE] .
- [51] C. Sgalletta, G. Iorio, M. Mapelli, M. C. Artale, L. Boco, D. Chattopadhyay, A. Lapi, A. Possenti, S. Rinaldi, and M. Spera, MNRAS **526**, 2210 (2023), arXiv:2305.04955 [astro-ph.HE] .
- [52] X. Xie, J. Zrake, and A. MacFadyen, Astrophys. J. **863**, 58 (2018), arXiv:1804.09345 [astro-ph.HE] .
- [53] The website of P. Freire lists 20 confirmed binary neutron star systems whose masses have been measured; see [50]

for a review. The mean value of the total mass in these 20 cases is  $(2.642 \pm 0.137)M_{\odot}$ . It may seem surprising that the range of total mass of BNS systems is so narrow, given that neutron star masses have been observed from as low as about  $1M_{\odot}$  to above  $2M_{\odot}$ , but neutron stars with masses significantly different from  $\approx 1.33M_{\odot}$  are generally paired with white dwarfs, normal stars or black holes, while the formation of a binary NS without disruption of the binary appears to occur only for a narrow mass range; see [51] for a discussion and population synthesis modeling of binary neutron stars.

- [54] The wide variation in the light curves of short GRBs does not contradict this; simulations constrained to the kilonova associated with the binary neutron star merger GW170817 show that the variation in the observed light curves of short GRBs is attributable to different viewing angles of the jet and different circumbinary medium [52].
- [55] An example relevant for this purpose is the detailed study of the Amaterasu particle reported in [2]. Existing codes to calculate energy losses during propagation do not treat higher masses than Fe but Ref. [34] gives an approximate treatment which suggests that nuclei heavier than iron may have energy-loss horizons considerably larger than Fe, which would be important in quantitatively interpreting abundances of extreme energy cosmic rays in future datasets.